"Donor−Two-Acceptor" Dye Design: A Distinct Gateway to NIR Fluorescence

Naama Karton-Lifshin,[†] Lorenzo Albertazzi,[‡,§] Michael Bendikov,[⊥] Phil S. Baran,[||] and Doron Shabat*[,†]

[†]School of Chemistry, Raymond and Beverly Sackler Faculty of Exact Sciences, Tel Aviv 69978, Israel

[‡]Institute for Complex Molecular Systems, Laboratory of Macromolecular and Organic Chemistry, Eindhoven University of Technology, P.O. Box 513, 5600 MB Eindhoven, The Netherlands
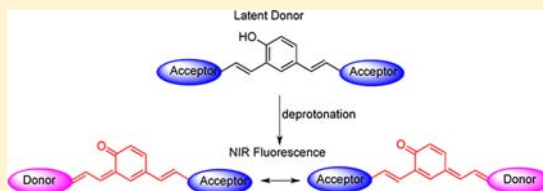
[§]NEST, Scuola Normale Superiore and Istituto Nanoscienze-CNR, I-56127 Pisa, Italy.

[⊥]Department of Organic Chemistry, The Weizmann Institute of Science, 76100 Rehovot, Israel.

[||]Department of Chemistry, The Scripps Research Institute, 10550 North Torrey Pines Road, La Jolla, California 92037, United States

S *Supporting Information*

ABSTRACT: The detection of chemical or biological analytes upon molecular reactions relies increasingly on fluorescence methods, and there is a demand for more sensitive, more specific, and more versatile fluorescent molecules. We have designed long wavelength fluorogenic probes with a turn-ON mechanism based on a donor–two-acceptor π-electron system that can undergo an internal charge transfer to form new fluorochromes with longer π-electron systems. Several latent donors and multiple acceptor molecules were incorporated into the probe modular structure to generate versatile dye compounds. This new library of dyes had fluorescence emission in the near-infrared (NIR) region. Computational studies reproduced the observed experimental trends well and suggest factors responsible for high fluorescence of the donor–two-acceptor active form and the low fluorescence observed from the latent form. Confocal images of HeLa cells indicate a lysosomal penetration pathway of a selected dye. The ability of these dyes to emit NIR fluorescence through a turn-ON activation mechanism makes them promising candidate probes for *in vivo* imaging applications.

INTRODUCTION

Fluorescence probe design is a rapidly expanding area of research in the chemical and biological sciences.[1,2] The detection of chemical or biological analytes in response to molecular changes relies increasingly on fluorescence,[3,4] and thus, there is a demand for more sensitive, more specific, and more versatile fluorescent molecules that can be used *in vivo*.[5] Such molecules must have high physiological stability, high quantum yields of fluorescence, long emission wavelengths, large Stokes shifts, and good photostability.[6−8] Most fluorescent probes were developed for *in vitro* use.[9,10] In order to apply fluorescent probes for *in vivo* imaging, one must consider the requirements for tissue optical penetration and the autofluorescence of biological molecules. Near-infrared (NIR) fluorescence has emerged as a tool for a broad spectrum of *in vivo* applications including nondestructive small animal imaging.[11−15] Because tissue absorbance and autofluorescence are significantly lower within this spectral range, NIR light can penetrate deep into tissues and provide useful diagnostic information[16,17] with specificity that makes it an attractive and less expensive alternative to classical radioisotope detection methods for molecular imaging. In this respect, we have recently developed a novel class of turn-ON NIR cyanine-based probes.[18] The probes are based on the new fluorochrome QCy7[19,20] (Figure 1), which is obtained upon removal of a specific trigger moiety by an analyte of interest. A distinctive
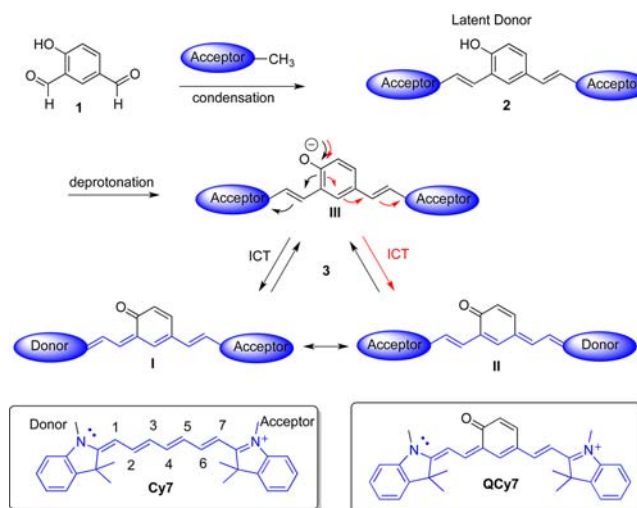

Figure 1. General synthesis and mechanism of activation of D2A cyanine-like fluorescence probes.

change of the π-electron system leads to generation of a cyanine dye with strong NIR fluorescence. The probe was used

to image endogenous hydrogen peroxide produced in an acute inflammation model in mice.[18] The synthetic strategy used to prepare the QCy7 fluorochrome is versatile and can be modularly utilized to obtain a novel family of fluorogenic compounds. Here we report a new library of NIR fluorescent molecular probes based on the distinctive donor−two-acceptor (D2A) rational design approach.

■ RESULTS AND DISCUSSION

Design, Synthesis and Fluorescence Measurements. The fluorescence of cyanine dyes is due to a polymethine π-electron system with a donor−acceptor pair between two nitrogen atoms. For instance, the fluorochrome of Cy7 (Figure 1) has one nitrogen atom with an electron pair as a donor moiety and a second positively charged nitrogen atom as an acceptor, bridged by a heptamethine π-electron chain. We have demonstrated use of a distinctive molecular design to introduce a turn-ON mechanism option in a cyanine molecule. As illustrated in Figure 1, the condensation of phenol-dialdehyde **1** with two equivalents of a general acceptor molecule affords dye compound **2**. This dye is composed of a phenol moiety that functions as a latent donor in conjugation with two acceptors. Deprotonation of the phenol leads to formation of a phenolate active donor **III** that is able to donate a pair of π-electrons to either one of the conjugated acceptors (structures **I** and **II** of compound **3**). This intramolecular charge transfer (ICT) generates a resonance species with a π-electron pattern similar to that of Cy7 fluorochrome. On the basis of calculations described below, structure **I** (Figure 1) is a preferred resonance structure, whereas structures **II** and **III** have less resonance contribution. The donor capability of the phenolate species **III** can be masked either by a proton or by a specific protecting group. Such a protected phenol can be used as a molecular probe for detection or imaging of an analyte that can react with the probe to remove the protecting group. The π-electron arrangement of structure **II** can be viewed as a general D2A system, and this dye family can be used to prepare probes with a turn-ON option.

A variety of molecules that function as π-electron acceptors can be incorporated in dye **2**, thereby creating a family of D2A dyes. Examples of possible acceptor-molecules with such capability are presented in Figure 2.
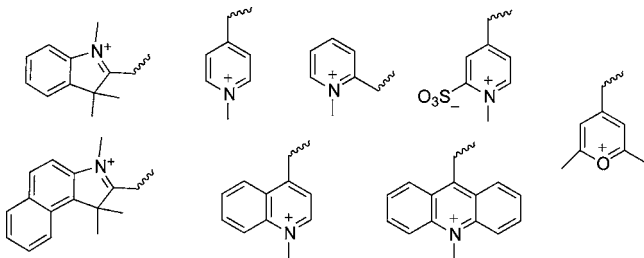

Figure 2. Chemical structure of potential acceptor moieties.

This approach can be further extended by replacing the donor moiety in dye **2** with two other phenol derivatives (Figure 3). Phenol **1a** can be condensed with two equivalents of a general acceptor molecule to afford dye compound **2a**, whereas phenol **1b** can be condensed with three equivalents of a general acceptor to produce dye compound **2b**. Deprotonation of phenols **2a** and **2b** generates the corresponded conjugated donor−acceptor pairs **4** and **5** with a new
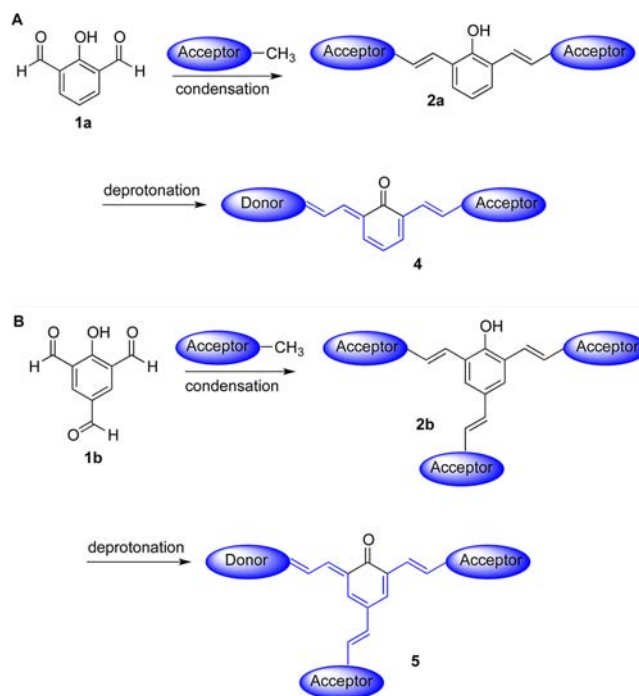

Figure 3. Preparation of (A) donor−two-acceptor and (B) donor−three-acceptor dye systems.

fluorochrome. The donor moiety can be condensed with either two identical acceptor molecules or with two different ones.

Following the described strategy, we synthesized a series of compounds to form a library of new dye molecules with a donor−two-acceptors or donor−three-acceptors mechanisms of action. The structures, and the corresponding spectroscopic data obtained for dye molecules prepared with donor **1**, donor **1a**, and donor **1b** are respectively presented in Tables 1, 2, and 3

The UV−vis and the fluorescent spectra of the dyes from this library support our prediction of obtaining NIR fluorescence through a D2A design. Spectra of representative dyes from each table are shown respectively in Figures 4, 5 and 6. The dye of entry 6 comprises a phenol latent donor and two different acceptors, a picolinium moiety and an indolium one (Figure 4). Deprotonation of the phenolic dye results in formation of a new donor−acceptor pair fluorochrome. The UV−vis spectrum exhibits a major absorption peak with a maximum at 550 nm, and the fluorescence spectrum indeed shows an emission peak in the NIR region at a wavelength of 650 nm.

The dye shown in entry 10 is composed of a phenol latent donor and two identical acceptors based on a picolinium moiety (Figure 5). Deprotonation of the phenolic form leads to formation of a new donor−acceptor pair fluorochrome. The UV−vis spectrum exhibits two absorption peaks with maxima at 330 and 490 nm, and the fluorescence spectrum shows an emission peak in the NIR region at a wavelength of 660 nm.

The dye shown in entry 18 is similarly composed of a phenol latent donor and three acceptors: two picolinium moieties and an indolium one (Figure 6). Deprotonation of the phenolic compound leads to formation of three resonance structures of new fluorochrome. The UV−vis spectrum exhibits an absorption peak with maximum at 550 nm, and the fluorescence spectrum shows an emission peak in the NIR region at a wavelength of 680 nm.

Table 1. Chemical Structures and Spectroscopic Data of Dyes Obtained from Donor 1

Entry	Dye structure	Donor	Acceptor	λex [nm]	λem [nm]	φ [%]	$\varepsilon \left[\dfrac{1}{M \cdot cm}\right]$
1				460 590	710	16	$\varepsilon_{480} = 42400$ $\varepsilon_{590} = 46000$
2				350 440	630	0.4	$\varepsilon_{350} = 14900$ $\varepsilon_{440} = 10550$
3				350 480 560	530 730	0.4	$\varepsilon_{350} = 12500$ $\varepsilon_{480} = 11500$ $\varepsilon_{560} = 11650$
4				350 460 540	730	0.6	$\varepsilon_{350} = 18500$ $\varepsilon_{460} = 18650$ $\varepsilon_{540} = 17800$
5				510 570	----	----	$\varepsilon_{510} = 16050$ $\varepsilon_{570} = 17100$
6				450 550	650	17	$\varepsilon_{450} = 23600$ $\varepsilon_{550} = 44400$
7				550	----	----	$\varepsilon_{550} = 20400$

This library of fluorophores offers choice of dye compounds with various characteristics. To demonstrate the potential advantage of such a library, we evaluated the aqueous stability of four selected compounds in comparison to that of the known NIR fluorophore, Cy7. The dyes were incubated in PBS (pH 7.4), at 37 °C, and the NIR fluorescent emission of each was monitored over 72 h (Figure 7). Three dyes had higher aqueous stability than that of Cy7 (dyes of entries 6, 10, and 18); entry-1 dye had stability similar to that of Cy7. Interestingly, dyes of entries 6 and 10 were highly stable; no loss of NIR fluorescence was observed even after 72 h.

As illustrated in Figure 1, the ICT from the phenolate donor to one of the two acceptor moieties leads to formation of a new fluorochrome with NIR fluorescence. Importantly, the protonated form of the dye (the phenol structure) does not emit fluorescence in the NIR region (see Supporting Information). Therefore, these dyes can be used as NIR fluorescence probes for determination of pH in aqueous solution in the region of the pK_a value of the phenols. The types of the acceptor moieties present in the dye molecule affect the pK_a of each phenol. To demonstrate this, the pK_a's of three dyes were measured by monitoring their emitted fluorescence as a function of the environmental pH (Figure 8). The phenols of dyes from entries 18, 10 and 6 had pK_a's of 2.9, 3.9, and 5.2, respectively.

The relative low pK_a values of our phenolic dyes emphasize that under physiological conditions, these dyes would be in a phenolate form. In an aqueous environment, the ICT mode of action will take place, and the dyes will emit NIR fluorescence.

Computational Study. In order to better understand the mechanism of NIR fluorescence from the **QCY7′**-type chromophore, we performed a computational study (at B3LYP/6-31G(d) level of theory, see Supporting Information for details) of the excitation and emission spectra of **CY7′**, **QCY7′**, protonated **QCY7′** (**QCY7H′**), **QCY7′** with elongated conjugation length (**QCY7CC′**), and **QCY7′** with electron-withdrawing groups (**QCY7F2′**), see Scheme 1. The results are summarized in Table 4.

Generally, the computations reproduced well the observed experimental trends and allowed the analysis of the factors responsible for high fluorescence of **QCY7′** and low fluorescence of the protonated form. The source of strong fluorescence is a conjugated backbone between the two acceptor units. This is evident by the very strong predicted fluorescence of the parent system (**CY7′**, Table 4). Once this conjugated backbone is interrupted by an aromatic ring, as in a protonated system (**QCY7H′**), fluorescence is weak. Shapes of the frontier orbitals of **CY7′** and **CY7H′**, given in Figure 9, also support this explanation. Indeed, LUMO of **CY7′** is located on a conjugated oligoene backbone, while conjugation in LUMO of **CY7H′** is partially interrupted by an aromatic ring. Additionally, the change in the orbital shape from HOMO to LUMO is relatively small in the backbone of **QCY7′** but is significantly larger in the case of protonated **QCY7H′** (Figure

Table 2. Chemical Structures and Spectroscopic Data of Dyes Obtained from Donor 1a

Entry	Dye structure	Donor	Acceptor	λex [nm]	λem [nm]	φ [%]	$\varepsilon \left[\dfrac{1}{M\cdot cm}\right]$
8				360 / 530	720	0.8	$\varepsilon_{360}=14240$ / $\varepsilon_{530}=8160$
9				340 / 520	720	2.9	$\varepsilon_{340}=26080$ / $\varepsilon_{520}=21520$
10				320 / 490	660	5	$\varepsilon_{320}=28040$ / $\varepsilon_{490}=22520$
11				400 / 570	760	0.6	$\varepsilon_{400}=26900$ / $\varepsilon_{570}=26900$
12				360 / 550	720	0.8	$\varepsilon_{360}=47300$ / $\varepsilon_{550}=37750$
13				350 / 530	720	2.6	$\varepsilon_{350}=38800$ / $\varepsilon_{530}=43133$
14				350 / 500	700	2	$\varepsilon_{350}=54733$ / $\varepsilon_{500}=48933$
15				330 / 490	640	7	$\varepsilon_{330}=32900$ / $\varepsilon_{490}=26100$
16				430	600	0.3	$\varepsilon_{420}=34800$

Table 3. Chemical Structures and Spectroscopic Data of Dyes Obtained from Donor 1b

Entry	Dye structure	Donor	Acceptor	λex [nm]	λem [nm]	φ [%]	$\varepsilon \left[\dfrac{1}{M\cdot cm}\right]$
17				350 / 490	710	0.3	$\varepsilon_{340}=38750$ / $\varepsilon_{490}=40800$
18				550	660	9	$\varepsilon_{550}=8700$
19				340 / 550	660	6	$\varepsilon_{340}=30000$ / $\varepsilon_{550}=44500$

9). This leads to a large Stokes shift and also to minimal fluorescence of the protonated form. Elongation of the π-bonding system by addition of two double bonds to the conjugated backbone (as in the **QCY7CC′**, Scheme 1 and
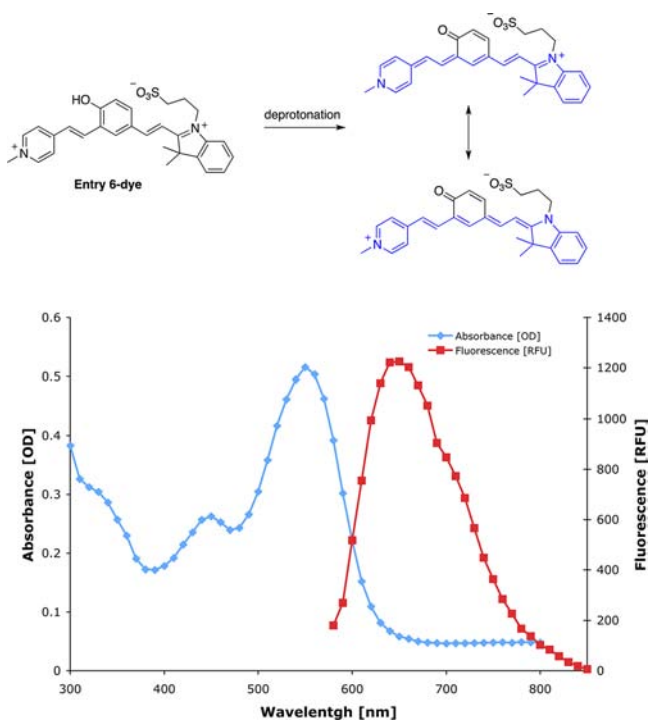
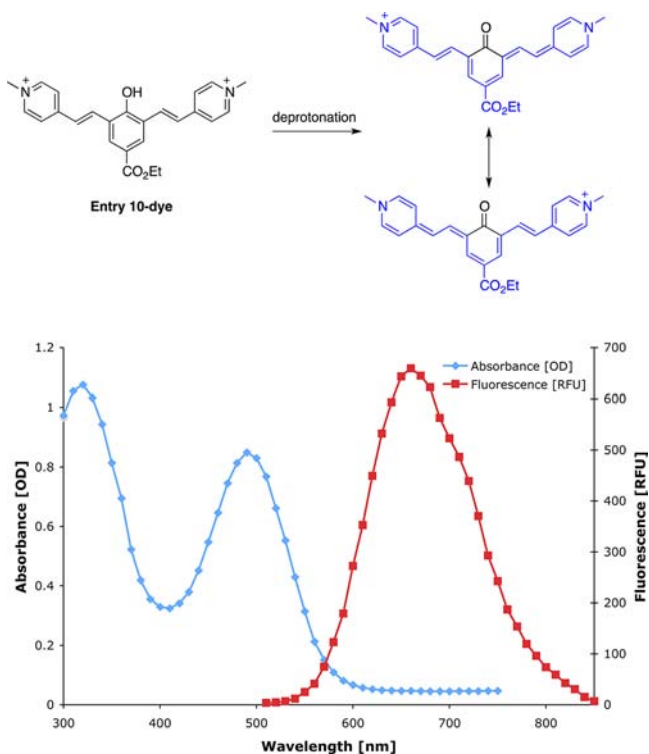**Figure 4.** Absorption and fluorescence spectra of entry-6 dye, 50 μM in PBS, pH 7.4.

Figure 5. Absorption and fluorescence spectra of entry-10 dye, 100 μM in PBS, pH 7.4.
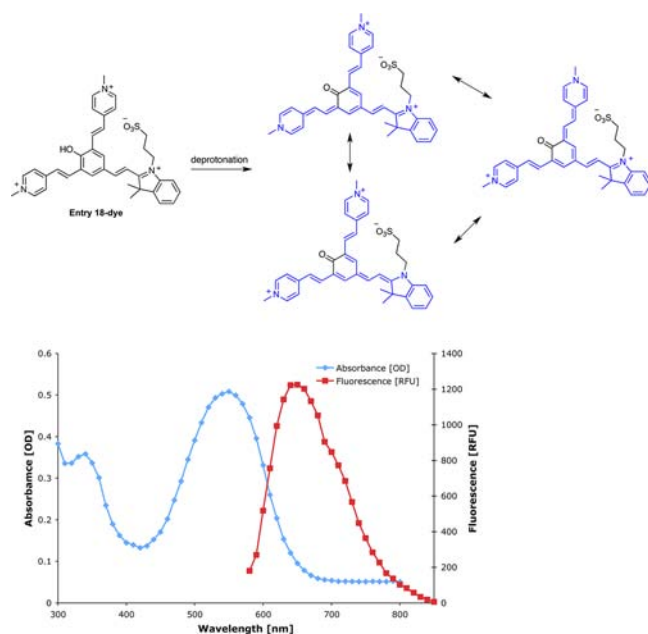

Figure 6. Absorption and fluorescence spectra of entry-18 dye, 50 μM in PBS, pH 7.4.

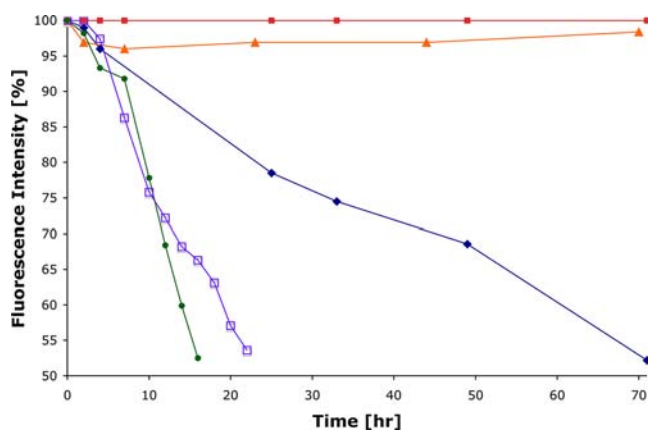**Figure 7.** Normalized intensity of NIR fluorescence emission for dyes entries 1 (green -··-), 6 (blue -◆-), 10 (red -■-), 18 (orange -▲-), and Cy7 (-□-) as a function of time (in PBS, pH 7.4, 37 °C).

Table 4) leads to even stronger fluorescence than predicted for the parent that is also significantly shifted toward the NIR region. Addition of an electron-withdrawing group on the aromatic ring (as in the **QCY7F2′**, Scheme 1 and Table 4) resulted in slightly weaker predicted fluorescence that is only slightly shifted toward the NIR region relative to that of the parent. Elongation of the conjugated backbone in Cy7 D2A systems is an excellent strategy to increase the fluorescence and to shift it to the NIR region, as also shown in experimental results given in Tables 1−3.

Confocal Fluorescent Images of Cells. Fluorogenic probes are useful for imaging various biological functions. Some of the newly synthesized dyes were found to have good cell permeability and were likely to generate *in vitro* fluorescent images. Figure 10 shows confocal images of HeLa cells incubated with dye 18. The accumulation of the dye in the lysosomal vesicles indicates cell penetration through endocytosis. As expected, the dye emitted NIR fluorescence even under the acidic conditions of the lysosome (pH ≈ 5). To further demonstrate the utility of the fluorophore for NIR *in vitro* imaging, cells were incubated with dye 18 overnight, washed, and imaged with a confocal microscope (Figure 10). The NIR fluorescence emitted by the dye indicates its chemical stability inside cells.
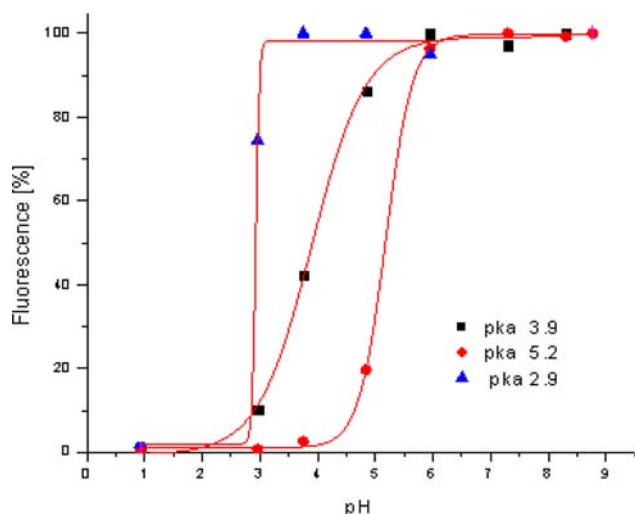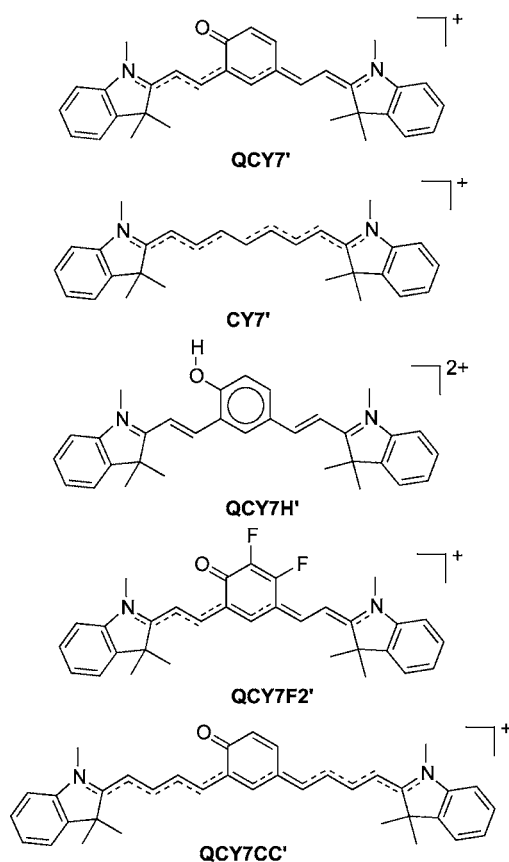

Figure 8. Determination of pK_a values for phenols of dyes shown in entries-6 (red -●-), -10 (black -■-) and -18 (blue -▲-). The pK_a's of the dyes were measured in various buffer solutions at the indicated pH. Buffer solutions preparation conditions: pH 1- KCl + HCl 0.2 M; pH 2−5 - AcOH + NaOH 0.1 M; pH 5−8.3 - PBS 0.1 M, pH 8.8 NaHCO$_3$ + NaOH 0.1 M. Fluorescence measurements wavelength: entries-6 and -18 dyes λ_{ex} = 550 nm, λ_{em} = 650 nm, entry-10 dye λ_{ex} = 490 nm, λ_{em} = 660 nm.

Scheme 1. Chemical Structures of Model Compounds Used in Calculations

Masking of the active phenol functional group of the dye molecules provides a convenient path to fluorescent probes with a turn-ON mode of action. Such probes can be used to detect an analyte of interest that reacts with the probe to result

Table 4. Calculated Absorption and Emission Transitions and Their Calculated Oscillator Strength for Selected D2A Systems Given in Scheme 1

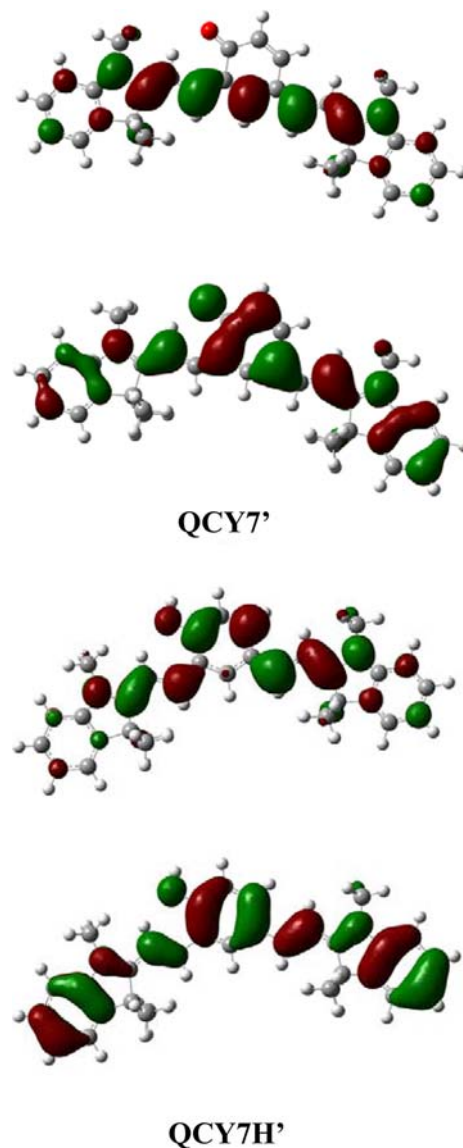|	$\lambda_{max,abs}$ (eV)	f_{abs}	$\lambda_{max,em}$ (eV)	f_{em}
QCY7′	2.20 eV (563 nm)	1.53	1.97 eV (629 nm)	1.02
CY7′	2.25 eV (550 nm)	2.46	2.08 eV (595 nm)	2.15
QCY7H′	2.65 eV (467 nm)	0.84	2.09 eV (595 nm)	0.13
QCY7CC′	1.87 eV (663 nm)	2.32	1.56 eV (792 nm)	1.17
QCY7F2′	2.16 eV (575 nm)	1.26	1.84 eV (672 nm)	0.68

Figure 9. Frontier orbital pictures. (Top two): **QCY7′** (LUMO and HOMO). (Bottom two): **QCY7H′** (LUMO and HOMO) calculated at B3LYP/6-31G(d) level.

in removal of the masking group. To demonstrate that the synthesized dyes could be incorporated into turn-ON probes, we synthesized probe **6**, a masked form of dye 10 (Figure 11). Reaction of hydrogen peroxide with the phenyl boronic acid protecting group caused release of the active dye.[21] Whereas probe **6** emitted fluorescence in the green region, dye 10 emitted in the NIR region. Therefore, the probe ratiometric activity can be used to image hydrogen in cells. An NIR laser was used to excite the sample at 820 nm to obtain two-photon
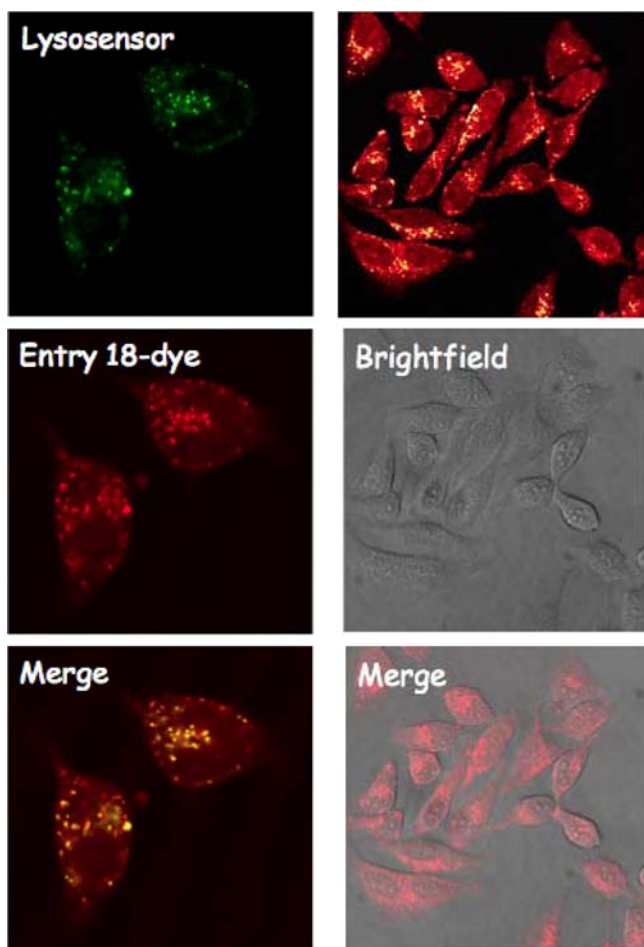
Figure 10. Confocal imaging of HeLa cells. (Images on left) Dye 18 co-localizes with the lysosome marker lysosensor, demonstrating that the dye is localized mainly in the lysosomal vesicles. (Images on right) Confocal images of HeLa cells incubated overnight with dye 18. Samples were excited with a 561-nm laser, and fluorescence was acquired in the range of 570−800 nm.

Figure 11. Two-photon imaging of hydrogen peroxide in living HeLa cells. HeLa cells were treated with probe **6** for 4 h at 37 °C, washed, and then treated with 1 mM of H_2O_2 or left untreated. Fluorescence from the caged compounds (green channel) and the uncaged dyes (red channel) was simultaneously acquired.

excitation. Cells were incubated with probe **6** for 4 h, washed, and treated with exogenous hydrogen peroxide. Figure 11 shows confocal images of HeLa cells incubated with probe **6** in the absence and in the presence of hydrogen peroxide. As expected, only green fluorescence was observed from the cells in the absence of hydrogen peroxide (the observed NIR fluorescence was negligible). However, in the presence of hydrogen peroxide, NIR fluorescence was observed. The enlarged photo of several cells provides strong indication of *in vitro* activation of the probe by hydrogen peroxide (see Supporting Information).

◼ DISCUSSION

The chromophores of most known fluorescent dyes have conjugated π-electrons and a push−pull structural element. The push component (the donor) is typically a heteroatom such as oxygen or nitrogen, while the pull component (the acceptor) can be any of various electron-withdrawing groups. Our dye molecules are composed of a phenol latent donor in conjugation with two acceptors. The latent donor is turned ON upon formation of a phenolate ion. The unique design enables an ICT from the activated donor to one of the two acceptors to form a 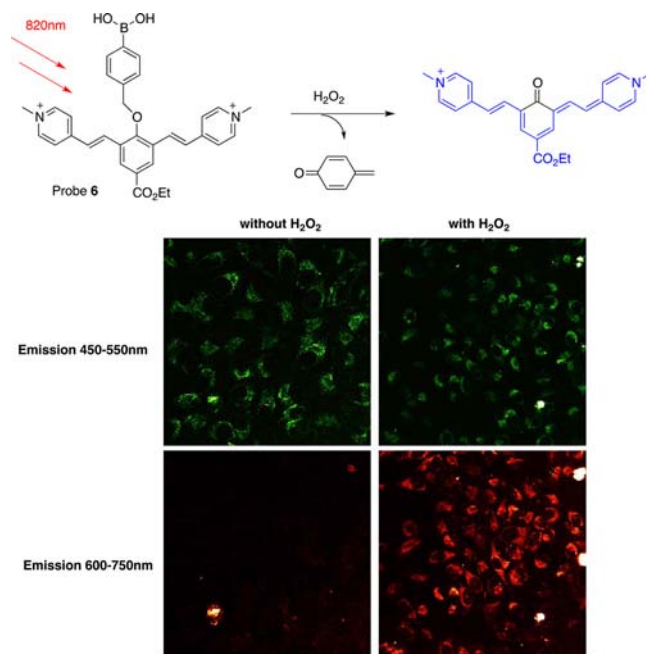new push−pull conjugated chromophore between the former two acceptors. The newly formed push−pull structural element has a larger π-system than that of the original donor−acceptor π-system and thus can emit fluorescence in longer wavelengths. Several electron-withdrawing groups were found to be good acceptors; however, only a phenolate acted as an efficient donor in our analysis. Attempts to incorporate an aniline functional group as a donor did not result in dyes that emitted noteworthy NIR fluorescence.

The Stokes shifts between the excitation and the emission wavelengths of about 150−200 nm observed for most of the new dyes are significantly larger those observed for the known cyanines such as Cy5 and Cy7 (10−20 nm). This larger Stokes shift is a desirable feature for fluorescence probes as it is correlated with a greater signal-to-noise ratio. Fluorescent dyes that absorb in wavelengths of 350−550 nm can be excited in the NIR region with a two-photon laser.[22] This option provides the advantages of NIR excitation for chromophores that do not absorb in the NIR range. To demonstrate the potential of dyes in our library to undergo a two-photon excitation with an NIR laser, dye 10 was evaluated. The dye exhibits a two-photon excitation spectrum in wavelengths between 800 and 1000 nm and therefore could be used to provide confocal cell images (see Supporting Information).

Cyanine molecules are considered to be among the most efficient NIR fluorophores. However, their chemical structure does not readily allow functionalization to mask their fluorescence in order to generate a turn-ON probe. Previous efforts to design such turn-ON probes typically had limitations of low fluorescence quantum yields, low extinction coefficients, and complex synthesis procedures.[23,24] Our approach allows us to mask a cyanine fluorochrome with various protecting groups and to release the active dye through the ICT mechanism. The modular chemical structure of the probe allowed us to prepare

a variety of masked cyanine dyes; all are equipped with the turn-ON mode of action. Of those tested, the use of indolium or picolinium groups as acceptors and phenol as a donor resulted in formation of dyes with the optimal spectroscopic characteristics, including long emission wavelength and quantum optical yield.

Predicting the fluorescence behavior of organic compounds solely on on the basis of chemical structure is not straightforward. Indeed, the relationship between the molecular structure and spectroscopic properties of the obtained dyes cannot always be fully understood since even subtle modifications can lead to fluorescence quenching through various pathways such as FRET (Förster resonance energy transfer), PET (photoinduced electron transfer), and more. The D2A-conjugated chromophore approach described here is without precedent since organic compounds are transformed into NIR fluorophores after initial ICT.

In order to understand how and why the fluorescence properties of the dyes are tuned by different acceptors, we have prepared a library of analogues and analyzed their absorbances and fluorescence spectra. In general, stronger acceptors produced dyes with higher quantum yield and longer fluorescence emission wavelength. For example, the indolium group is known to be a stronger acceptor than a picolinium one. In entry 1 (Table 1), the dye is equipped with two indolium acceptors, whereas in entry 2, the dye has two picolinium acceptors. Accordingly, the fluorescence emission of entry-1 dye is observed at a longer wavelength (710 nm) than that of entry-2 dye (630 nm). Following this trend, dye 1 had a quantum yield of 16%, whereas the quantum yield of dye 2 is only 0.4%. In the case of the dye in entry 5 (Table 1), where the acceptor is the more powerful pyrilium species, the failure to fluoresce is due to the chemical instability under aqueous conditions. Thus, it can be concluded that, barring chemical instability, the acceptor ability of the D2A system can be used to qualitatively predict the fluorescence capabilities.

Within the D2A dye system, the electrophilic nature of the ortho-acceptor is another significant factor that affects fluorescence properties. Thus, those derivatives bearing an indolium acceptor at the ortho position underwent a slow spiro-cyclization to form spirocyanine III (Figure 12). The
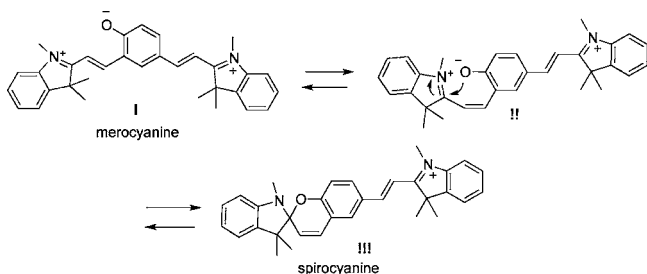

Figure 12. Merocyanine–spirocyanine reversal transformation.

spiro-derivative can no longer function as a D2A fluorophore. Although this transformation is reversible, such derivatives exhibited faster lost of the NIR fluorescence in comparison to their counterparts with a picolinium acceptor (see Figure 7).

To summarize, the new donor–acceptor π-electron system reported here produces NIR fluorescence emission with good and, as mentioned above, often predictable spectroscopic characteristics. Collectively, the studies of how the donor and acceptor units interact (structure–activity relationships) are

also supported by computation. Specifically, the addition of electron-withdrawing groups on the aromatic ring and the elongation of the π-electron system are predicted to result in shifted emission wavelength toward the NIR region. Indeed, such characteristics are observed empirically when using hydrolytically stable, stronger π-electron acceptors.

CONCLUSIONS

In summary, we have developed a novel strategy for design of long-wavelength fluorogenic probes. Our design is based on a D2A π-electron system that can undergo an ICT to form a new fluorochrome with a longer π-conjugated system. Several different latent donors and multiple acceptor molecules were incorporated into the probe modular structure to generate versatile dye compounds. This strategy was demonstrated by synthesis of a new library of dyes that had fluorescence emission in the NIR region. Masking of the phenolate donor, by a proton or an analyte-induced functional-group inter-conversion, provided a convenient route for obtaining a turn-ON probe. As with other fluorogenic dyes, our new probes could be used to monitor various functions in cells. A computational study supported the observed experimental trends and allowed analysis of the factors responsible for high fluorescence of the D2A active form and the low fluorescence observed from the latent form as well as factors responsible for shift of the fluorescence into NIR region. Confocal images of HeLa cells indicated that the tested dye penetrates cells through the lysosomal pathway. Such probes can be used as pH sensors or for detection of specific analytes that have cleavage reactivity for the phenolate-masking group. The ability of these dyes to emit NIR fluorescence through a turn-ON activation mechanism makes them promising candidate probes for *in vivo* imaging applications. We anticipate that our unique strategy will open a new door for further NIR fluorescence probe discovery.

ASSOCIATED CONTENT

S **Supporting Information**

Full experimental details, characterization data of all new compounds, description of computational methods, spectro-scopic assay conditions, and *in vitro* experimental conditions. This material is available free of charge via the Internet at http://pubs.acs.org.

AUTHOR INFORMATION

Corresponding Author
chdoron@post.tau.ac.il
Notes
The authors declare no competing financial interest.

ACKNOWLEDGMENTS

■ REFERENCES

(1) Hangauer, M. J.; Bertozzi, C. R. *Angew. Chem., Int. Ed.* **2008**, *47*, 2394−2397.

(2) Lee, S.; Park, K.; Kim, K.; Choi, K.; Kwon, I. C. *Chem. Commun.* **2008**, 4250−4260.

(3) Kobayashi, H.; Ogawa, M.; Alford, R.; Choyke, P. L.; Urano, Y. *Chem. Rev.* **2010**, *110*, 2620−2640.

(4) Weissleder, R.; Tung, C. H.; Mahmood, U.; Bogdanov, A., Jr. *Nat. Biotechnol.* **1999**, *17*, 375−378.

(5) Reymond, J. L.; Fluxa, V. S.; Maillard, N. *Chem. Commun.* **2009**, 34−46.

(6) Hirayama, T.; Van de Bittner, G. C.; Gray, L. W.; Lutsenko, S.; Chang, C. J. *Proc. Natl. Acad. Sci. U.S.A.* **2012**, *109*, 2228−2233.

(7) Johnsson, N.; Johnsson, K. *ACS Chem. Biol.* **2007**, *2*, 31−38.

(8) Kim, E.; Koh, M.; Lim, B. J.; Park, S. B. *J. Am. Chem. Soc.* **2011**, *133*, 6642−6649.

(9) Redy, O.; Kisin-Finfer, E.; Sella, E.; Shabat, D. *Org. Biomol. Chem.* **2012**, *10*, 710−715.

(10) Weinstain, R.; Segal, E.; Satchi-Fainaro, R.; Shabat, D. *Chem. Commun.* **2010**, *46*, 553−555.

(11) Ebert, B.; Riefke, B.; Sukowski, U.; Licha, K. *J. Biomed. Opt.* **2011**, *16*, 066003.

(12) Lee, H.; Akers, W.; Bhushan, K.; Bloch, S.; Sudlow, G.; Tang, R.; Achilefu, S. *Bioconjugate Chem.* **2011**, *22*, 777−784.

(13) Licha, K.; Olbrich, C. *Adv. Drug Delivery Rev.* **2005**, *57*, 1087−1108.

(14) Licha, K.; Resch-Genger, U. *Drug Discovery Today: Technol.* **2012**, *8*, 87−94.

(15) (a) Yuan, L.; Lin, W.; Yang, Y.; Chen, H. *J. Am. Chem. Soc.* **2012**, *134*, 1200−1211;(b) *J. Am. Chem. Soc.* **2012**, *134*, 13510−13523.

(16) Blum, G.; von Degenfeld, G.; Merchant, M. J.; Blau, H. M.; Bogyo, M. *Nat. Chem. Biol.* **2007**, *3*, 668−677.

(17) Pham, W.; Choi, Y.; Weissleder, R.; Tung, C. H. *Bioconjugate Chem.* **2004**, *15*, 1403−1407.

(18) Karton-Lifshin, N.; Segal, E.; Omer, L.; Portnoy, M.; Satchi-Fainaro, R.; Shabat, D. *J. Am. Chem. Soc.* **2011**, *133*, 10960−10965.

(19) Karton-Lifshin, N.; Presiado, I.; Erez, Y.; Gepshtein, R.; Shabat, D.; Huppert, D. *J. Phys. Chem. A* **2012**, *116*, 85−92.

(20) Presiado, I.; Karton-Lifshin, N.; Erez, Y.; Gepshtein, R.; Shabat, D.; Huppert, D. *J. Phys. Chem. A* **2012**, *116*, 7353−7363.

(21) Lippert, A. R.; De Bittner, G. C. V.; Chang, C. J. *Acc. Chem. Res.* **2011**, *44*, 793−804.

(22) Hanninen, P.; Soukka, J.; Soini, J. T. *Ann. N.Y. Acad. Sci.* **2008**, *1130*, 320−326.

(23) Ho, N. H.; Weissleder, R.; Tung, C. H. *Bioorg. Med. Chem. Lett.* **2006**, *16*, 2599−2602.

(24) Richard, J. A.; Massonneau, M.; Renard, P. Y.; Romieu, A. *Org. Lett.* **2008**, *10*, 4175−4178.